

# Theoretical analysis of the heat convection coefficient in large vessels and the significance for thermal ablative therapies

Luisa Consiglieri<sup>1</sup>, Icaro dos Santos<sup>2</sup> and Dieter Haemmerich<sup>3</sup>

<sup>1</sup> Department of Mathematics and CMAF, University of Lisboa, Av Prof Gama Pinto 2, 1649-003, Lisboa, Portugal

<sup>2</sup> Department of Electrical and Computer Engineering, University of Texas at Austin, C0803, Austin, TX 78712, USA

<sup>3</sup> Department of Surgery, University of Wisconsin-Madison, 600 Highland Av CSC H4/725, Madison, WI 53792, USA

E-mail: icaro@ieee.org

Received 26 August 2003

Published 5 December 2003

Online at [stacks.iop.org/PMB/48/4125](http://stacks.iop.org/PMB/48/4125)

## Abstract

Ablative therapies such as radio-frequency (RF) ablation are increasingly used for treatment of tumours in liver and other organs. Often large vessels limit the extent of the thermal lesion, and cancer cells close to the vessel survive resulting in local tumour recurrence. Accurate estimates of the heat convection coefficient  $h$  for large vessels will help improve ablation techniques, and are required for estimation of thermal lesion dimensions in simulations. Previous estimates of  $h$  did not consider that only part of the vessel is heated, and assumed uniform temperature distribution at the vessel wall. An analytical relationship between the heat convection coefficient, blood velocity and temperature is formulated. The heat convection coefficient evaluated will assist both simulations and design of proper protocols for *in vivo* measurements. The mathematical model developed in this work describes the exchange of heat between a solid surface and a moving fluid and it is based on energy and motion equations for Navier–Stokes fluids. A particular case of a laminar blood flow in the portal vein is studied when a portion of its surface is heated. The results show that heating a larger portion of the vessels reduces convective heat loss, which may result in more effective ablation strategies.

## 1. Introduction

Different ablative therapies are clinically used to treat liver cancer, as well as tumours in kidney, bone and lung (Goldberg *et al* 1998a, Vanderschueren *et al* 2002, Gervais *et al* 2003, Dupuy *et al* 2000). Microwave, laser and ultrasound are used to heat tissue, but worldwide

the most widely used method is radio-frequency (RF) ablation. Therefore, this work will concentrate on RF ablation, even though this study is applicable to other thermal ablative therapies. During RF ablation a thin electrode is placed directly into the tumour using ultrasound, computed tomography or magnetic resonance imaging guidance. A RF generator creates electric current in the tissues through the electrodes. The tumour is heated due to the Joule effect causing necrosis of the malignant cells once tissue temperature exceeds around 50 °C. Consequently, if the technique is successful it might cure the patient.

One limitation of thermal ablative therapies is the heat sink effect caused by large vessels. Radio-frequency ablation coagulates vessels up to 3 mm diameter, but larger vessels remain perfused. Cancer cells close to these vessels may not reach required temperatures, survive, and result in local tumour recurrences.

It has been shown that tumour recurrence occurs more frequently when the hepatic tumour is localized next to a vessel (Goldberg *et al* 1998a). So far strategies to alleviate the heat sink effect of large vessels have concentrated on reducing blood flow by either pharmacologic agents (Goldberg *et al* 1998b) or by occluding hepatic inflow (i.e. occlusion of the blood in the portal vein, celiac artery or hepatic artery) (Chinn *et al* 2001). The temperature profile in the liver tissue and, hence, the size of the lesion is very dependent on the heat convection coefficient  $h$  in these vessels, which describes the heat sink effect (Haemmerich *et al* 2003). Since  $h$  is the parameter that has a significant impact on the shape of the lesion obtained during hepatic RF ablation, an important step towards the improvement of the RF ablation is the prediction of  $h$ . The overall objective of this work is to study and theoretically predict the values of  $h$  in the hepatic vessels during RF ablation. A better understanding of the behaviour of  $h$  will help guide experiments, improve numerical simulations and design better protocols for the hepatic RF ablation.

In order to predict  $h$ , a correlation equation is developed. The equation presented here describes the convective heat transfer when only a portion of the surface of a vessel is heated. As will be shown, this is a more realistic situation for ablation techniques than correlation equations used in previous work where a fully thermally developed condition is assumed. Furthermore, the results of this study can be applied to any organ where large vessels limit the extent of thermal lesion formation, e.g., for liver and kidney cancer treatment.

## 2. Estimate of $h$ that has been used in previous work

A number of previous studies examine heat transfer in blood vessels. Charm *et al* (1968) experimentally investigated heat transfer in small tubes (0.6 mm diameter) in a water bath.

Victor and Shah calculated heat transfer for uniform heat flux and uniform wall temperature cases for fully developed flow (Victor and Shah 1975), and in the entrance region (Victor and Shah 1976).

Legendijk (1982) calculated temperature distributions in the entrance region around large vessels during hyperthermia, assuming laminar and fully thermally developed flow.

Chato (1980) developed correlation equations for estimating the heat transfer under different configurations and diameters of blood vessels.

Barozzi and Dumas (1991) calculated heat transfer in the entrance region considering the rheological blood properties, and a cell-depleted plasma layer at the vessel wall.

Kolios *et al* (1995) used conservation of energy equations for calculating temperature profiles around large vessels, since heat transfer coefficients change during temperature changes, and may vary circumferentially.

Tungjatkusolmun *et al* (2002) modelled the influence of a large vessel on thermal lesion formation during RF ablation, and assumed constant vessel wall temperature.

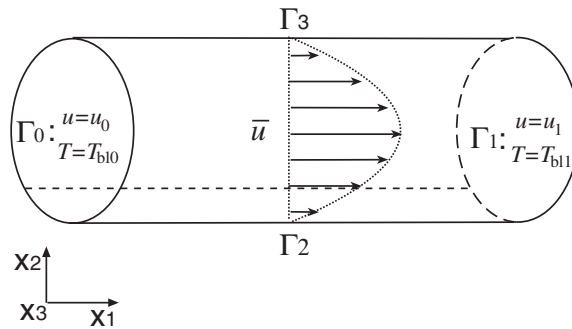


Figure 1. Laminar flow inside the hepatic vessel. The boundary conditions are indicated.

Haemmerich *et al* (2003) improved the model used by Tungjitkusolmun *et al* and used estimates of the heat transfer coefficient to model the effect of a large vessel on thermal lesion formation during RF ablation, assuming fully thermally developed flow. However, only a small region of the vessel is heated during ablative procedures, and the fully thermally developed condition is not attained.

For application to thermally ablative therapies, partial heating of the vessel must be considered, which has not been done in previous work. Furthermore, constant heat flux, constant wall temperature or fully thermally developed flow cannot be assumed as was done in previous work. In this work the heat transfer coefficient is calculated, considering heating of a large vessel in part of its surface, and part of its circumference. Later a non-uniform temperature profile along the heated vessel region is considered. Section 3 presents in detail the development of the analytical expression for the prediction of  $h$ .

### 3. The analytical model

In this section, using the classical theory of fluid mechanics and heat transfer, a relationship between the heat convection coefficient, fluid velocity and temperature in the boundaries is formulated. When investigating heat transfer in blood vessels, typically the non-Newtonian rheological behaviour of blood, as well as a cell-depleted plasma layer at the vessel wall must be considered. The rheological behaviour of blood enhances heat transfer, but only significantly for vessels smaller than 0.5 mm diameter (Barozzi and Dumas 1991). Similarly, the plasma layer must be only considered for small vessels (Charm *et al* 1968). This work investigates large vessels and assumes Newtonian fluid behaviour.

A domain  $\Omega \subset \mathbb{R}^n$  ( $n = 2$  or  $3$ ) representing the portal vein (figure 1) is considered. The boundary is  $\partial\Omega = \bar{\Gamma}_0 \cup \bar{\Gamma}_1 \cup \bar{\Gamma}_2 \cup \bar{\Gamma}_3$ , where  $\Gamma_0$ ,  $\Gamma_1$ ,  $\Gamma_2$  and  $\Gamma_3$  are open subsets of  $\partial\Omega$ , not intersecting each other, which represent fictional walls where the blood flow begins and ends, the zone of contact with the ablated zone and the surrounding boundary where it is assumed that the flow is adherent to the surface, respectively.

The blood flow can be described as an incompressible Navier–Stokes fluid governed by its equation of motion

$$\rho \left( \frac{\partial \mathbf{u}}{\partial t} + (\mathbf{u} \cdot \nabla) \mathbf{u} \right) - \nabla \cdot (\mu(T) \nabla \mathbf{u}) = \nabla p \text{ in } \Omega \quad (1)$$

and the incompressibility condition

$$\nabla \cdot \mathbf{u} = \sum_{i=1}^n \frac{\partial u_i}{\partial x_i} = 0 \quad (2)$$

where  $\mathbf{u} = (u_i)_{i=1, \dots, n}$  represents the blood velocity,  $\rho$  is the density,  $T$  is the temperature,  $\mu$  is the viscosity and  $p$  is the pressure. The boundary conditions are

$$\mathbf{u} = \mathbf{u}_0 \quad \text{on } \Gamma_0 \quad (3)$$

$$\mathbf{u} = \mathbf{u}_1 \quad \text{on } \Gamma_1 \quad (4)$$

$$\mathbf{u} = \mathbf{0} \quad \text{on } \Gamma_2 \cup \Gamma_3 \quad (5)$$

where  $\mathbf{u}_0$  and  $\mathbf{u}_1$  are known. The initial condition is  $\mathbf{u}(0) = \mathbf{u}_0$ .

The temperature satisfies the energy equation and initial and boundary conditions

$$\rho c_p \left( \frac{\partial T}{\partial t} + \mathbf{u} \cdot \nabla T \right) - \nabla \cdot (k(T) \nabla T) = \mu(T) |\nabla \mathbf{u}|^2 \quad \text{in } \Omega \quad (6)$$

$$T(x, 0) = T_{bl0} \quad x \in \Omega \quad (7)$$

$$T = T_{bl0} \quad \text{on } \Gamma_0 \quad (8)$$

$$T = T_{bl1} \quad \text{on } \Gamma_1 \quad (9)$$

$$k(T) \frac{\partial T}{\partial n} = h(T_s - T) \quad \text{on } \Gamma_2 \quad (10)$$

$$k(T) \frac{\partial T}{\partial n} = 0 \quad \text{on } \Gamma_3 \quad (11)$$

where  $c_p$  is the specific heat,  $k$  is the thermal conductivity of the blood,  $T_{bl0}$  is a constant blood temperature,  $T_{bl1}$  is the temperature at the vessel outlet (and could be experimentally determined),  $h$  is the convective heat transfer coefficient and  $T_s$  is the temperature of the heated region at the vessel wall.

Equation (10) is the so-called Newton law of cooling.

Multiplying (1) by the blood velocity  $\mathbf{u}$ , and integrating in space, it follows that

$$\rho \int_{\Omega} \frac{\partial \mathbf{u}}{\partial t} \cdot \mathbf{u} \, dx + \rho \int_{\Omega} (\mathbf{u} \cdot \nabla) \mathbf{u} \cdot \mathbf{u} \, dx - \int_{\Omega} \nabla \cdot (\mu(T) \nabla \mathbf{u}) \cdot \mathbf{u} \, dx = \int_{\Omega} \nabla p \cdot \mathbf{u} \, dx. \quad (12)$$

Considering the incompressibility condition (2) and the boundary condition (5), integrating by parts the convective term as well as the right-hand side of the last equation, both these terms vanish. Then equation (12) implies

$$\rho \int_{\Omega} \frac{\partial \mathbf{u}}{\partial t} \cdot \mathbf{u} \, dx + \int_{\Omega} \mu(T) |\nabla \mathbf{u}|^2 \, dx = \int_{\Gamma_0 \cup \Gamma_1} \mu(T) \sum_{i,j=1}^n \frac{\partial u_i}{\partial x_j} u_i n_j \, d\Gamma. \quad (13)$$

On the other hand, integrating (6) in space, it follows that

$$\rho c_p \int_{\Omega} \frac{\partial T}{\partial t} \, dx + \rho c_p \int_{\Omega} \mathbf{u} \cdot \nabla T \, dx - \int_{\Omega} \nabla \cdot (k(T) \nabla T) \, dx = \int_{\Omega} \mu(T) |\nabla \mathbf{u}|^2 \, dx. \quad (14)$$

Recalling the divergence theorem

$$\int_{\Omega} \nabla \cdot (k(T) \nabla T) \, dx = \int_{\partial \Omega} k(T) \frac{\partial T}{\partial n} \, d\Gamma$$

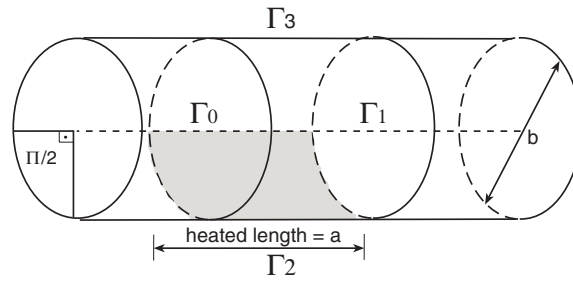


**Figure 2.** Representation of the simulated vessel. The length  $a$  is the portion of the vessel that is heated during the RF hepatic ablation.

and using the boundary conditions (8)–(11), equation (14) becomes

$$\rho c_p \int_{\Omega} \left( \frac{\partial T}{\partial t} + \mathbf{u} \cdot \nabla T \right) dx = \int_{\Gamma_2} h(T_s - T) d\Gamma + \int_{\Omega} \mu(T) |\nabla \mathbf{u}|^2 dx. \quad (15)$$

At the steady-state case, taking into account equation (13) equation (15) leads to

$$\rho c_p \int_{\Omega} \mathbf{u} \cdot \nabla T dx = \int_{\Gamma_2} h(T_s - T) d\Gamma + \int_{\Gamma_0 \cup \Gamma_1} \mu(T) \sum_{i,j=1}^n \frac{\partial u_i}{\partial x_j} u_i n_j d\Gamma. \quad (16)$$

Moreover, taking into account the relation

$$\int_{\Omega} \mathbf{u} \cdot \nabla T dx = \int_{\partial\Omega} \mathbf{u} \cdot \mathbf{n} T d\Gamma - \int_{\Omega} \nabla \cdot \mathbf{u} T dx$$

and recalling the incompressibility condition (2) and the boundary conditions (3)–(5), equation (16) yields

$$\int_{\Gamma_2} h(T_s - T) d\Gamma = \rho c_p \int_{\Gamma_0 \cup \Gamma_1} \mathbf{u} \cdot \mathbf{n} T d\Gamma - \int_{\Gamma_0 \cup \Gamma_1} \mu(T) \sum_{i,j=1}^n \frac{\partial u_i}{\partial x_j} u_i n_j d\Gamma. \quad (17)$$

Note that the last term on the right-hand side of equation (17) vanishes, when a laminar flow is considered. Consequently, this relationship allows the calculation of  $h$  or at least the mean value of  $h$  in relation to the values of velocity and temperature of the blood appearing only on the boundaries. Since these values on the boundaries can be determined, the relation allows a more accurate evaluation of  $h$ .

Section 4 shows how to apply equation (17) in order to evaluate  $h$  in a large vessel. Three cases are considered in detail.

#### 4. Heat transfer in the portal vein

In this section, equation (17) is used for qualitatively and quantitatively studying the heat flux behaviour in some particular cases in the portal vein.

##### 4.1. Case 1

Consider a laminar Navier–Stokes fluid  $\mathbf{u}(\mathbf{x}) = (u(x_2, x_3), 0, 0)$  as in figure 2, which has a constant mean value  $\bar{u}$  of the fluid velocity on  $\Gamma_0$  and  $\Gamma_1$ .

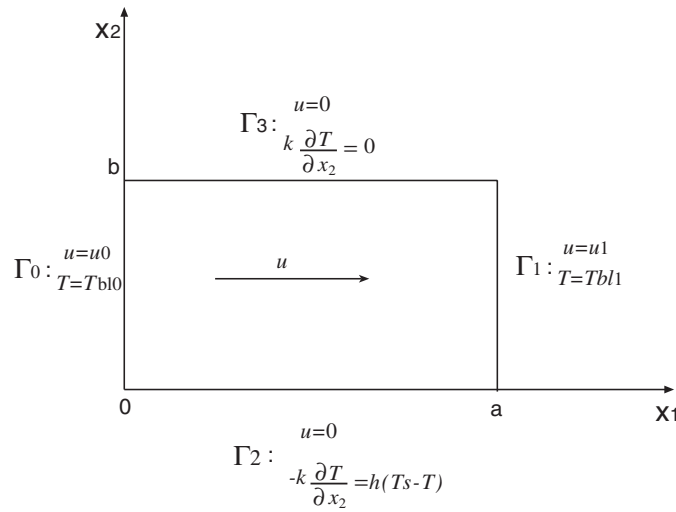


Figure 3. Laminar Navier–Stokes fluid in the plane.

In order to calculate  $h$ , equation (17) can be reduced to

$$\bar{h} = \frac{\rho c_p \int_{\Gamma_0 \cup \Gamma_1} \mathbf{u} \cdot \mathbf{n} T \, d\Gamma}{(T_s - T_m) |\Gamma|} = \rho c_p \frac{\bar{u} (T_{b1} - T_{b0}) b}{(T_s - T_m) a} \quad (18)$$

where  $\bar{h}$  is the average heat convection coefficient,  $T_m$  is  $\frac{T_{b0} + T_{b1}}{2}$  and  $|\Gamma|$  is the measure of  $\Gamma$ . In this case, it is assumed that one quarter of the circumference is heated by the RF catheter, that is,  $|\Gamma_0| = |\Gamma_1| = \pi b^2/4$  and  $|\Gamma| = a\pi b/4$ .

In this case, in the integral equation (17) constant average temperatures are considered before calculation. It will be shown later in section 5 that this simplification causes virtually no error in the evaluation of  $h$ . On the other hand, this simplification reduces computational calculations, which facilitates the implementation of real-time data acquisition systems based on microcontrollers.

#### 4.2. Case 2

In order to compare results from equation (17) with the pointwise Newton law of cooling (10), the problem is formulated in a two-dimensional cross-section perpendicular to  $x_3$ . Considering a laminar Navier–Stokes fluid  $\mathbf{u}(\mathbf{x}) = (u(x_1, x_2), 0)$  in the plane (figure 3), equations (2) and (17) are reduced to

$$\frac{\partial u}{\partial x_1} = 0 \Leftrightarrow u(x_1, x_2) = u(x_2) \quad (19)$$

$$\bar{h} = \frac{\rho c_p \int_0^b (u_1(x_2) T(a, x_2) - u_0(x_2) T(0, x_2)) \, dx_2}{T_s a - \int_0^a T(x_1, 0) \, dx_1}. \quad (20)$$

For both viscosity  $\mu$  and thermal conductivity  $k$  constants, the coupled system of differential equations (1) and (6) in the steady-state case

$$-\mu \frac{\partial^2 u}{\partial x_2^2} = p'(x_1) \quad (21)$$

$$\rho c_p u \frac{\partial T}{\partial x_1} - k \Delta T = \mu^2 \left| \frac{\partial u}{\partial x_2} \right|^2 \quad (22)$$

can be calculated. From equation (21) the flow becomes the well-known Poiseuille flow (Landau and Lifshitz 1987)

$$u(x_2) = -6 \frac{\bar{u}}{b^2} x_2 (x_2 - b).$$

Since the effect of friction is very small when compared to the other heat transfer mechanisms during the RF ablation procedure, the energy dissipation term in equation (22) is negligible. Furthermore, it is assumed that  $\frac{\partial^2 T}{\partial x_1^2}$  is small with respect to  $\frac{\partial^2 T}{\partial x_2^2}$ . Taking into account that  $T(0, 0) = T_{bl0}$ ,  $T(a, 0) = T_{bl1}$  and  $\frac{\partial T}{\partial x_2}(x_1, b) = 0$ , a solution of equation (22) is

$$T(x_1, x_2) = T_{bl0} + \frac{T_{bl1} - T_{bl0}}{a} x_1 - \frac{\bar{u}}{b^2} \frac{T_{bl1} - T_{bl0}}{a \chi} \left( \frac{x_2^4}{2} - b x_2^3 \right) - \frac{\bar{u}(T_{bl1} - T_{bl0})b}{a \chi} x_2$$

where  $\chi = k/(\rho c_p)$ . Consequently, the mean value of the heat convection coefficient can be calculated from (20) resulting as

$$\bar{h} = \rho c_p \frac{\bar{u}(T_{bl1} - T_{bl0})b}{(T_s - T_m)a}. \quad (23)$$

Although this formula is calculated from explicit solutions, note that this result coincides to (18) which is obtained taking into account the averages  $T_{bl0}$  on  $\Gamma_0$ ,  $T_{bl1}$  on  $\Gamma_1$  and  $T_m$  on  $\Gamma_2$ .

In this case, since there are explicit solutions,  $h$  can be determined pointwise. Using (10), it follows

$$h(x_1) = \frac{\rho c_p \bar{u}(T_{bl1} - T_{bl0})b}{(T_s - T_{bl0})a - (T_{bl1} - T_{bl0})x_1}.$$

For this pointwise result, the mean value of  $h$  is

$$\bar{h} = \frac{1}{a} \int_0^a h(x_1) dx_1 = -\frac{\rho c_p \bar{u}b}{a} \log \frac{T_s - T_{bl1}}{T_s - T_{bl0}}. \quad (24)$$

### 4.3. Case 3

During thermal ablation the vessel is not heated uniformly along its length. Regions close to the tip of the probe reach a higher temperature than other regions. Equation (17) can account for this behaviour. In order to exemplify the use of this equation, the temperature profile described in (25) is used

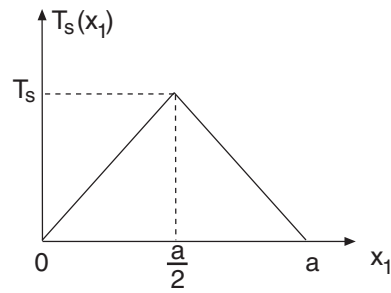
$$T_s(x_1) = \begin{cases} T_{bl0} + 2(T_s - T_{bl0})x_1/a & \text{if } 0 \leq x_1 \leq a/2 \\ T_{bl1} + 2(T_s - T_{bl1})(a - x_1)/a & \text{if } a/2 \leq x_1 \leq a. \end{cases} \quad (25)$$

Figure 4 is a graphical representation of this temperature profile.

Then, the mean value of the heat convection coefficient is

$$\bar{h} = \rho c_p \frac{\bar{u}(T_{bl1} - T_{bl0})b}{\frac{a}{2} \left( \frac{T_{bl0} + T_s}{2} + \frac{T_s + T_{bl1}}{2} \right) - T_m a}. \quad (26)$$

Numerical simulations based on the expressions obtained in this section and using experimental data obtained elsewhere are performed in section 5.



**Figure 4.** Simulated temperature profile of the heated region.

**Table 1.** Simulation parameters.

$T_{bl0}$	$T_{bl1}$	$T_s$	$b$	$\rho$	$c_p$
37 °C	37.05 °C	50 °C	1 cm	1000 Kg m <sup>-3</sup>	4180 J Kg <sup>-1</sup> °C <sup>-1</sup>

## 5. Numerical simulations and discussion

In the simulation, the diameter of the vessel is 10 mm, which is a typical diameter of the portal vein (Gray *et al* 1990). The inlet temperature of the vessel is the normal blood temperature, i.e., 37 °C. The simulated temperature in the heated region of the vessel is 50 °C because temperatures above 50 °C result in necrosis (Lounsberry *et al* 1995). As the primary concern is with areas close to the vessel not being destroyed and resulting in local tumour recurrence, the highest sublethal temperature is chosen as vessel wall temperature. During the ablation, only a small region of the vessel is heated. In the simulations, lengths of 2 cm and 3 cm of the vessel are heated (see figure 2). Later, different flow velocities are considered. A range of velocities from normal mean flow velocity in the portal vein (approximately 0.2 m s<sup>-1</sup> (Cioni *et al* 1992)) to almost total occlusion of the vein (0.01 m s<sup>-1</sup>) are simulated. To estimate the temperature difference between inlet and outlet flow ( $\Gamma_0$  and  $\Gamma_1$ , respectively) the work of Torrel and Nilson (1978) is used. In that work a graphical solution of the heat transfer equation is presented. This solution allows estimation of the fluid temperature along the tube axis, while part of the tube length is heated. When the whole circumference of the vein is heated the estimated temperature difference  $T_{bl1} - T_{bl0}$  is around 0.1 °C. In this work, only a quarter of the circumference ( $\pi/2$  rad) is heated. Therefore, a conservative estimate of 0.05 °C is used for this temperature difference.

A word of caution is necessary here. In the work of Torrel and Nilson (1978), neither the velocity nor the thermal boundary layer is developed, which is a valid assumption for thermal ablation. However, in their work the tube is uniformly heated, whereas in this study only part of the circumference is heated. Due to these limitations the temperature difference  $T_{bl1} - T_{bl0}$  used in the following calculations is a crude estimate. For a more accurate calculation of  $h$  using the results presented in this work, further experimental measurements of the temperature difference  $T_{bl1} - T_{bl0}$  are required.

Numerical simulations for cases 1 and 2 are presented (equations (18) and (24)). Recall that equations for  $\bar{h}$  in cases 1 and 2 differ when calculated directly from explicit solutions of motion and energy equations. The simulation parameters are shown in table 1. For the range of temperature and flow simulated here, equations (18) and (24) yield to virtually the same

**Table 2.** Simulation of cases 1 and 2.

Velocity (m s <sup>-1</sup> )	$h$ (W m <sup>-2</sup> K <sup>-2</sup> ) ( $a = 2$ cm)	$h$ (W m <sup>-2</sup> K <sup>-2</sup> ) ( $a = 3$ cm)
0.01	81	54
0.05	403	268
0.10	805	537
0.15	1208	805
0.20	1611	1074

values of  $h$ . Therefore, there is no error in considering  $h$  as a constant average convective heat transfer for this case. Hence, table 2 shows the results for both cases. Furthermore, due to the lack of experimental measurements for the temperature difference, case 3 is not presented here.

The simulation shows three important results. The first result is the fact that  $h$  varies considerably with both the flow rate and the length of the heated vessel region. This result may lead to improved ablation strategies for tumours located next to large vessels. Different catheter types that heat a longer region next to the vessel could be used. For ablative therapies where multiple probes can be used (e.g., microwave ablation, laser ablation), one could place another probe upstream from the tumour and thereby reduce the heat sink effect facilitated by the vessel.

The second result deals with measurement protocols. If direct measurements of  $h$  are necessary due to uncertainties in the flow and temperature profiles, one must either heat a region that has the size of the lesion to be achieved or calibrate the instrumentation to account for this behaviour.

Finally, the third result has consequences for mathematical modelling of RF ablation and other thermally ablative therapies. In order to accurately model thermal ablation, different values of  $h$  should be used as boundary conditions for different thermal lesion sizes.

## 6. Conclusion

Analytical equations for estimating the behaviour of  $h$  in vessels during thermally ablative therapies were developed. The heat transfer coefficient was estimated under the assumption of laminar flow. Numerical simulations were performed based on these equations, which showed that not only the flow rate in the vessel but also the size of the heated vessel region have a major impact in the heat convection coefficient. The results found here may help develop more accurate mathematical models of ablative therapies, measurement techniques, and improve clinical ablation procedures.

## References

- Barozzi G S and Dumas A 1991 Convective heat transfer coefficients in the circulation *J. Biomech. Eng.* **113** 308–13
- Charm S, Paltiel B and Kurland G S 1968 Heat transfer coefficients in blood flow *Biorheology* **5** 133–45
- Chato J C 1980 Heat transfer to blood vessels *Trans. ASME* **102** 110–8
- Chinn S B, Lee F T Jr, Kennedy G D, Chinn C, Johnson C D, Winter T C III, Warner T F and Mahvi D M 2001 Effect of vascular occlusion on radiofrequency ablation of the liver: results in a porcine model *Am. Roentgen Ray Soc.* **176** 789–95
- Cioni G, D'Alimonte P, Cristani A, Ventura P, Abbati G, Tincani E, Romagnoli R and Ventura E 1992 Duplex-doppler assessment of cirrhosis in patients with chronic compensated liver disease *J. Gastroenterol. Hepatol.* **7** 282–84

- Dupuy D E, Zagoria R J, Akerley W, Mayo-Smith W W, Kavanagh P V and Safran H 2000 Percutaneous radiofrequency ablation of malignancies in the lung *Am. J. Roentgenol.* **174** 57–9
- Gervais D A, McGovern F J, Arellano R S, McDougal W S and Mueller P R 2003 Renal cell carcinoma: clinical experience and technical success with radio-frequency ablation of 42 tumors *Radiology* **226** 417–24
- Goldberg S N, Gazelle G S, Solbiati L, Livraghi T, Tanabe K K, Hahn P F and Mueller P R 1998a Ablation of liver tumors using percutaneous rf therapy *Proc. 19th Int. Conf. IEEE Engineering in Medicine and Biology Society* vol 170 pp 1023–8
- Goldberg S, Hahn P, Halpern E, Fogle R and Gazelle G S 1998b Radiofrequency tissue ablation: effect of pharmacological modulation of blood flow on coagulation diameter *Radiology* **209** 761–7
- Gray S 1990 *Grays Anatomy* (New York: Vintage Books)
- Haemmerich D, Wright A S, Mahvi D M, Lee F T Jr and Webster J G 2003 Hepatic bipolar radiofrequency ablation creates lesions close to blood vessels—a finite element study *Med. Biol. Eng. Comput.* **41** 317–23
- Kolios M C, Sherar M D and Hunt J W 1995 Large blood vessel cooling in heated tissues: a numerical study *Phys. Med. Biol.* **40** 477–94
- Lagendijk J J W 1982 The influence of blood flow in large vessels on the temperature distribution in hyperthermia *Phys. Med. Biol.* **27** 17–23
- Landau L D and Lifshitz E M 1987 *Fluid Mechanics Course of Theoretical Physics* (Oxford: Pergamon)
- Lounsbury W, Goldschmidt V and Linke C 1995 The early histologic changes following electrocoagulation *Gastrointest. Endosc.* **41** 68–70
- Torrel L M and Nilson S K 1978 Temperature gradients in low-flow vessels *Phys. Med. Biol.* **23** 106–17
- Tungjitkusolmun S, Staelin T, Haemmerich D, Tsai J-Z, Cao H, Webster J G, Lee F T Jr, Mahvi D M and Vorperian V R 2002 Three-dimensional finite-element analysis for radio-frequency hepatic tumor ablation *IEEE Trans. Biomed. Eng.* **49** 3–9
- Vanderschueren G M, Taminiau A H, Obermann W R and Bloem J L 2002 Osteoid osteoma: clinical results with thermocoagulation *Radiology* **224** 82–6
- Victor S A and Shah V L 1975 Heat transfer to blood flowing in a tube *Biorheology* **12** 361–8
- Victor S A and Shah V L 1976 Steady state heat transfer to blood flowing in the entrance region of a tube *Int. J. Heat Mass Transfer* **19** 777–83